Molecular Crystals and Liquid Crystals Science and Technology. Section A. Molecular Crystals and Liquid Crystals

Publication details, including instructions for authors and subscription information:
http://www.tandfonline.com/loi/gmcl19

Liquid Crystal Alignment on Polymer Films

Ruibo Lu [a], Keshu Xu [a], Shengʹan Xiao [a], Yongkang Le [a], Xuewu Zhou [a], Haiming Wu [b], Jianhua Gu [b] & Zuhong Lu [b]

[a] Fudan—T.D. Lee Physics Laboratory, Laboratory of Laser Physics and Optics, Fudan University, Shanghai, 200433, China

[b] National Laboratory of Molecular and Biomolecular Electronics, Southeast University, Nanjing, 210018, China

Version of record first published: 24 Sep 2006

To cite this article: Ruibo Lu, Keshu Xu, Shengʹan Xiao, Yongkang Le, Xuewu Zhou, Haiming Wu, Jianhua Gu & Zuhong Lu (1998): Liquid Crystal Alignment on Polymer Films, Molecular Crystals and Liquid Crystals Science and Technology. Section A. Molecular Crystals and Liquid Crystals, 325:1, 51-62

To link to this article: http://dx.doi.org/10.1080/10587259808025383

Mol. Cryst. Liq. Cryst., Vol. 325, pp. 51–62
Reprints available directly from the publisher
Photocopying permitted by license only

Liquid Crystal Alignment on Polymer Films

RUIBO LU[a,*], KESHU XU[a], SHENG'AN XIAO[a], YONGKANG LE[a], XUEWU ZHOU[a], HAIMING WU[b], JIANHUA GU[b] and ZUHONG LU[b]

[a] *Fudan–T.D. Lee Physics Laboratory, Laboratory of Laser Physics and Optics, Fudan University, Shanghai 200433, China;*
[b] *National Laboratory of Molecular and Biomolecular Electronics, Southeast University, Nanjing 210018, China*

(Received 26 February 1997; In final form 18 March 1998)

The rubbed polyimide (PI) and PI LB films were fabricated and treated to align the nematic liquid crystal (LC) 5CB. The rubbed polyimide (PI) films aligned LC cell shows a higher LC pretilt angle than the cell aligned by PI LB films. Atomic force microscope (AFM) observations indicate that the rubbed PI films have a needle-like structure, while PI LB films have a groovy structure. We think that the needle-like structure plays a major role in producing the higher LC pretilt angle.

Keywords: Liquid crystal; alignment; polyimide; atomic force microscope

1. INTRODUCTION

A uniform and orderly liquid crystal (LC) alignment is a prerequisite for the preparation of a high quality liquid crystal device [1]. The rubbing polymer method is widely used for the commercial purpose to get homogeneous alignment [2]. As a rubbing-free technique, Langmuir–Blodgett (LB) method has aroused quite a lot interest for its monolayer scaled control of film thickness [3, 4]. No matter what kind of alignment treatment is adopted, it is essential that we obtain an appropriate LC pretilt angle through the application of the alignment procedure. For example, super-twisted nematic (STN) devices need a 5° to 20° pretilt angle to avoid the

*Corresponding author. Phone: 021-65492222 ext. 2374, Fax: 021-65642374; e-mail: 960187@ms.fudan.sh.cn

stripe instability [5]. Surface-stabilized ferroelectric liquid crystal (SSFLC) devices need a several degree pretilt angle to eliminate the zig-zag defects that may deteriorate the eletro-optic characteristics [6]. Therefore, it is important to elucidate the corresponding LC mechanism involved in them from both the theoretical and practical view. In order to understand the mechanism, it is meaningful to investigate the LC aligning films directly with high resolution. The emergence of atomic force microscope (AFM) has proved to be a powerful tool in this area for its atomic level resolution [7–10]. Even though some work has been done to investigate the rubbed polymer films and LB films, few reports are concerned about their different alignment ability. In this paper, we used both the rubbed polyimide (PI) and PI LB films to align nematic liquid crystal molecules and characterized the topological properties of the corresponding films by AFM. According to the AFM observations, we propose a possible underlying mechanism that causes the different LC alignment configurations.

2. EXPERIMENTAL

The polymer molecular structure used in this study is shown in Figure 1. Two different kinds of PI films were prepared from the corresponding polyamic acid with an average molecular weight of 6×10^4 (Product from Applied Chemistry Department, Shanghai Jiaotong University, China). One is the rubbed polyimide (PI) films. The polyamic acid solution with a polymer concentration of 1 wt% was firstly spin-coated onto the indium tin oxide (ITO) glass substrates. The spinning speed was 2000 rpm. The substrates were prebaked at 100°C for one hour, then pre-imidized at 150°C for another hour. After that, the substrates were cooled down to the room temperature for the rubbing process. The substrate surfaces were unidirectionally rubbed under a moving, velvet-coated cylinder at the constant force of 10 gf/cm. This is also a standard process used in the mass production. A further imidization was applied later at the temperature of 200°C for one more hour.

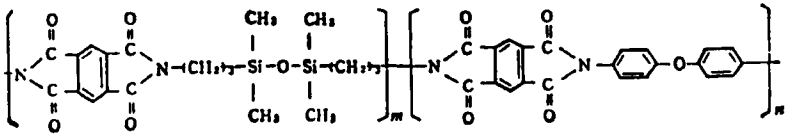

FIGURE 1 The polymer molecular structure of the polyimide compound.

The other type film is PI LB films. Since the polyamic acid shows no obvious amphiphilic properties, it is not appropriate for depositing LB films onto the substrates directly. So, a polyamic acid alkylamide salt (PAAS) was previously transferred as the precursor of PI LB films. The PAAS solution was a mixture of the polyamic acid and *N*, *N*-dimethylhexadecylamine in the molecular ratio 1:4 using *N*, *N*-dimethylacetamide and benzene 1:1 as the solvent. The concentration is 1.0 mM. The PAAS solution was spread onto the distilled water subphase and compressed at the air–water interface. At the surface pressure of 25 mN/m, the PAAS was deposited onto the ITO substrate by the vertical depositing method and five layers were transferred. After a similar imidization process as the rubbed PI films, the desired PI LB films were obtained.

The AFM (Nanoscope III, Digital Instruments) observations of the rubbed PI films and multilayer LB films were carried out on the ITO substrates at the temperature of 20°C in the air. The constant force mode was applied between the tip and the film surface. A 12.5 μm scanner was used for the large area scanning and a 0.7 μm scanner for the molecular resolution images. The force was on the order of 10 nN.

The sandwiched type LC cells were assembled along the antiparallel-rubbed surface direction for the rubbed films or with the depositing direction antiparallel for the PI LB films. The cell distance was controlled to be 25 μm. LC material 4-*n*-pentyl-4′-cyanobiphenyl (5CB) was injected into the cells when heated above the isotropic point, then cooled down slowly into the nematic phase under the vacuum. The pretilt angle of LCs was measured by the crystal rotation method [11].

3. RESULTS AND DISCUSSION

Figure 2 shows the typical isotherm curve between the molecular area and the surface pressure of PAAS on the air–water interface. The curve indicated that PAAS has a steep condensed region ranging from 15 to 45 mN/m for film deposition. So, it is appropriate for choosing 25 mN/m as the transferring surface pressure. It can also be seen from the curve that the limiting area per monomer unit was 0.92 nm^2.

The polarized microscope was used to observe the LC alignment in the cells. Both types of LC cells showed a uniform monodomain and no obvious nematic textures appeared rotating the cells under the polarized microscope. It indicates that the treated films have a good anchoring ability to align the

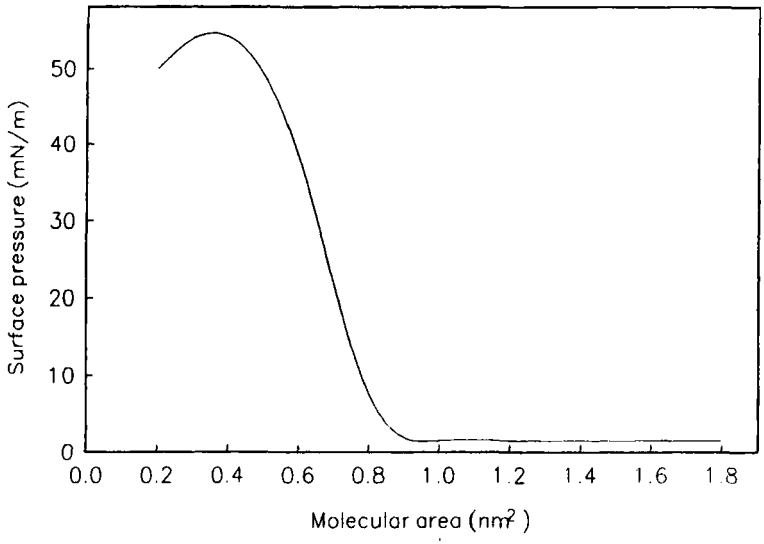

FIGURE 2 The isotherm curve between the molecular area and the surface pressure of PAAS at the temperature of 18°C.

LC molecules. The measured LC pretilt angle of the rubbed PI films aligned cell is 7°, while that of the PI LB films aligned cell is about 1°.

We first imaged a non-rubbed polymer surface for the comparison aim. At the scanning size of $4 \times 4\,\mu m$, an uneven surface topology can be observed as shown in Figure 3a. From this figure, one can see that the polymer molecules form irregular domains with a diameter ranging from several nanometer to 0.1 μm. The three dimensional (3D) image in Figure 3b reveals that the surface is an island-like domain region, which is different, as shown below, from the rubbed surface even though the irregular domains are still present after the rubbing process.

Figure 4a is a typical topological image of the rubbed films obtained by AFM. The scanning size is $11.1 \times 11.1\,\mu m$. Obvious scratches can be seen on the film even though they are not always parallel to each other along the rubbing direction. The randomly distributed spots, which are bright on the image, were regarded as deformed spherical shape clusters by Kim *et al.* [9]. From Figure 4b, the corresponding 3D topological image of Figure 4a, we could find that the clusters show a needle-like structure erecting out of the film surface with the average height around 9 nm. Under the zoom scale of $3 \times 3\,\mu m$ (Fig. 5a), the section analysis reveals that the root mean square (RMS) roughness of the structure is 1.9 nm as shown in Figure 5b. Similar

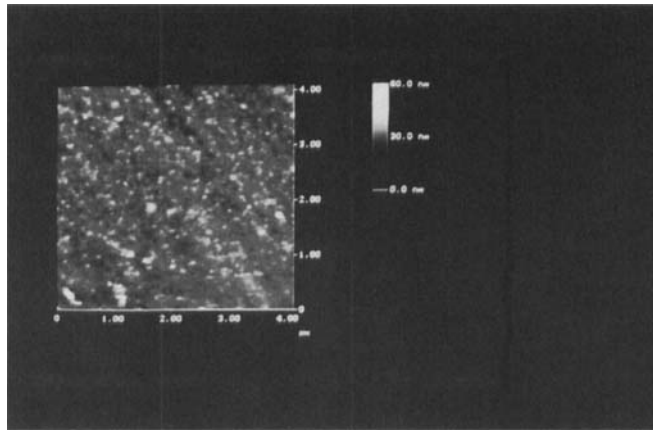

(a)

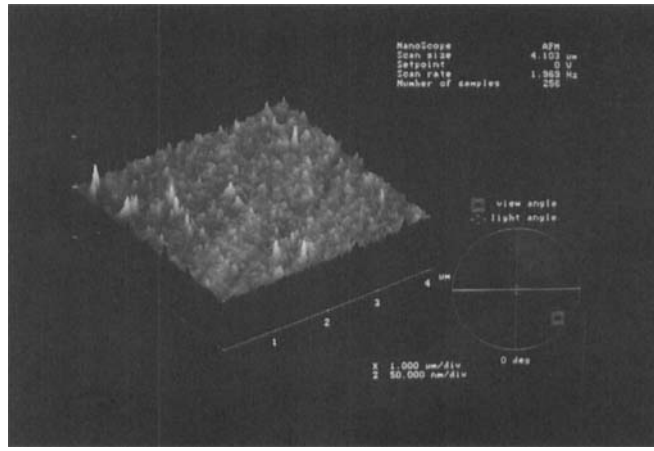

(b)

FIGURE 3 AFM image (a) and the corresponding 3D topological image (b) of the non-rubbed films under the microscale observation. The scanning size is $4.5 \times 4.5\,\mu m$. (See Color Plate III).

phenomena and results, as described above, can be got with good reproducibility when the tip scanned at different regions.

The existence of the needle-like structure may be from the free of rubbing after the further imidization. On the other part, since a weak rubbing has been employed in the pre-imidized period, the polymer films can be modified by the mechanical force without eliminating the clusters as under a hard rubbing [8]. In addition, our polymer sample has the properties of easy

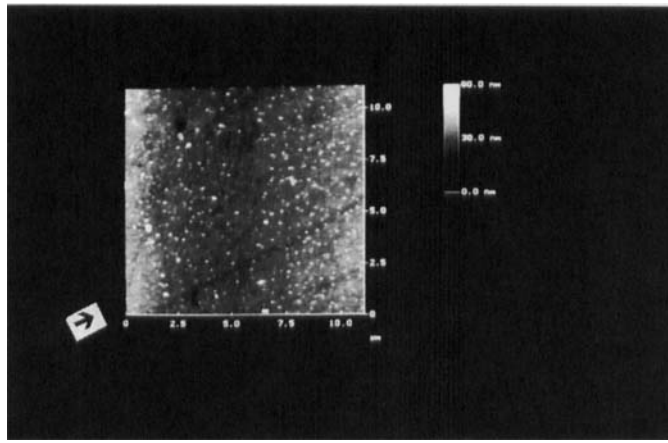

(a)

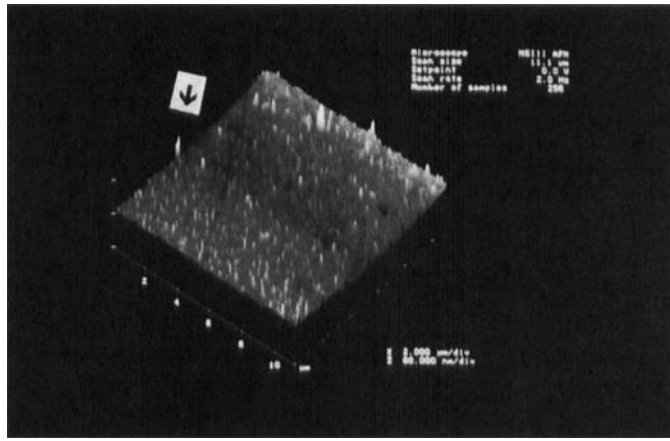

(b)

FIGURE 4 AFM image (a) and the corresponding 3D topological image (b) of the rubbed films under the microscale observation. The scanning size is $11.1 \times 1.11\,\mu m$. The rubbing direction is shown by the arrow. (See Color Plate IV).

crystallization. So, it is possible that the polymer balls formed by the polymer chains in the solution can be crystallized to stand out of the substrate surface during the heating process even with a rubbing process after the pre-imidization.

Figure 6a is a scanned image of the multilayer LB films on the ITO substrate ($4.5 \times 4.5\,\mu m$). The bright streaks correspond to the PAAS imidized PI LB films. The streaks are nearly oriented along the depositing

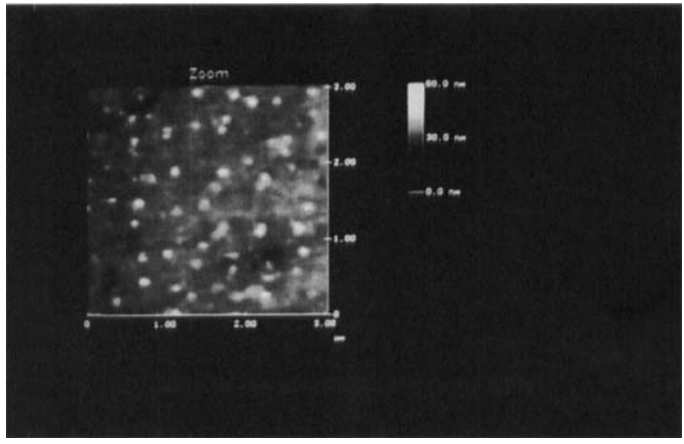

(a)

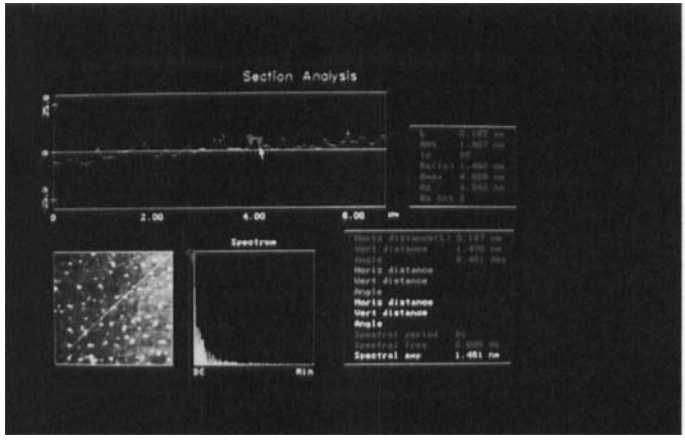

(b)

FIGURE 5 The zoom of AFM image in Figure 4a at the size of $3 \times 3\,\mu m$ (a) and its corresponding section analysis (b). (See Color Plate V).

direction though the streaks has an evident width difference ranging from 20 nm to more than 100 nm. The streaks therefore can not be judged as PI chains but as PI aggregates. The 3D image in Figure 6b revealed that the PI aggregates have a groovy surface between the neighboring ones with an average depth of 35 nm. When we further scanned a certain groovy surface down to the nanometer scale (4.4×4.4 nm), a molecular scale polymer structure was observed as shown in Figure 7. The image was stable during the tip probing process and similar images were also observed when different

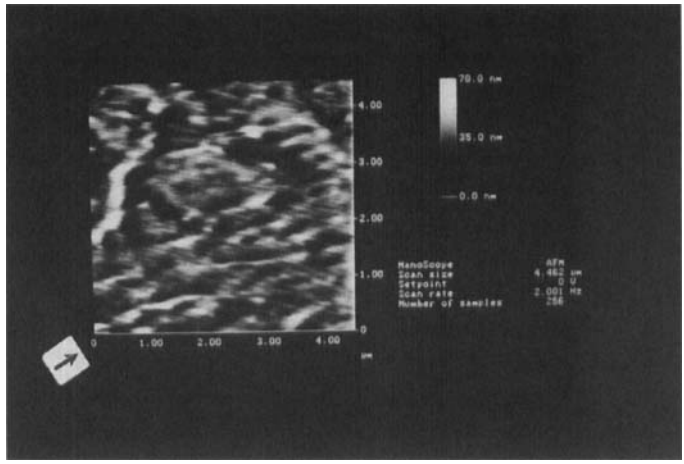

(a)

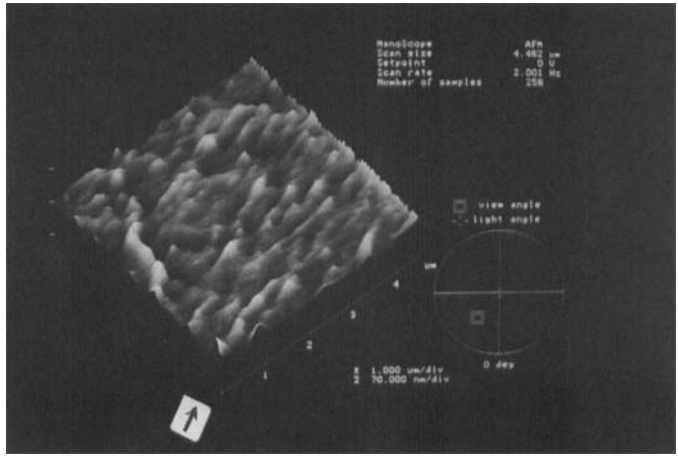

(b)

FIGURE 6 AFM image (a) and the corresponding 3D topological image (b) of the LB films under the microscale observation. The scanning size is $4.5 \times 4.5\,\mu m$. The film depositing direction is shown by the arrow. (See Color Plate VI).

positions were selected on the substrate for the investigation, which indicates that the images are not artifacts and can disclose the nano-scaled information of the deposited LB films. The little twisted structure is believed to be a polymer chain because it has an average chain width of 0.2 nm and a chain-to-chain distance of 0.48 nm that are consistant with the molecular dynamics calculation [12]. The chains are on the whole in-line oriented

along the depositing direction that probably comes from the vertical film deposition.

A scratch-free region of the rubbed films was also further scanned under a nanometer level (27×27 nm) as shown in Figure 7. An orderly in-line nanometer structure is discernible that is similar to the case of the LB films. Unfortunately, the oriented structure can not be definitely determined to be a single polymer chain because it has a chain width of 1.2 nm and a chain-to-chain distance of 1.8 nm that are both larger than the LB film nanostructure. This kind of polymer chains was along the rubbing direction, which may come from the polymer film rearrangement induced by the rubbing procedure [13] .

It has been known that the success of any surface-induced alignment method depends on the orderliness of the aligning films introduced by the substrate, the aligning material and the film treatment procedure employed. According to the alignment mechanism theory of the chemical and physical interactions, there are four factors that contribute to the LC alignment at the LC/substrate interface, which are the dispersive, the polar, the steric and the topological interactions [14]. Except for the topological part, the other three contributions are mainly governed by the intermolecular interactions between the substrate and the LC. Which interaction is dominant under a particular aligned system depends on the prevailing circumstances and finally determines the LC pretilt angle in the cell. Under the nanoscale AFM investigation, both the rubbed PI films and the LB films showed an orderly

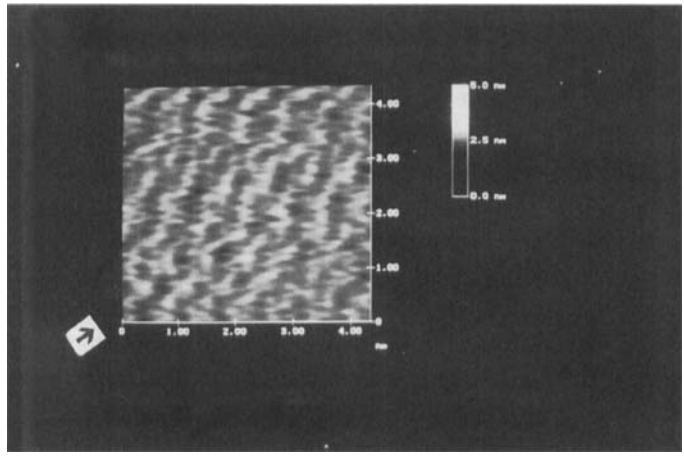

FIGURE 7 AFM image of the LB films under the nanoscale observation. The scanning size is 4.4×4.4 nm. The arrow indicates the film depositing direction. (See Color Plate VII).

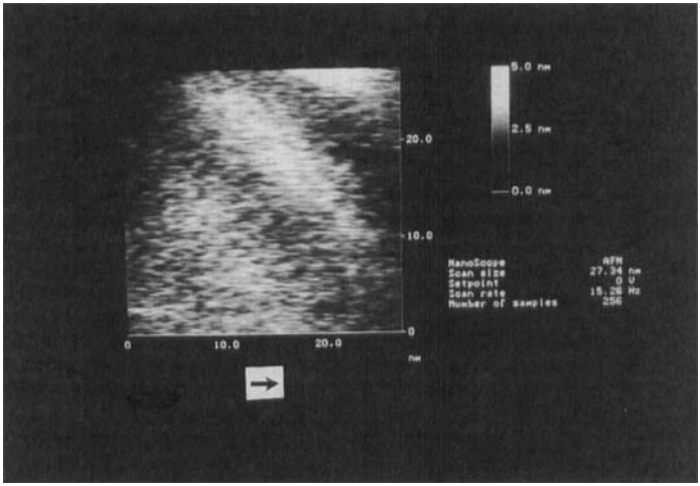

FIGURE 8 AFM image of the rubbed films under the nanoscale observation. The scanning size is 27 × 27 nm. The arrow indicates the rubbing direction. (See Color Plate VIII).

in-line polymer chain structure along either the rubbing direction or the LB film depositing direction, which was caused or oriented by the film preparing procedure. So, the orderliness of the polymer chains can induce the LC molecules to align along a certain direction which derives from the intermolecular interactions concerning about the dispersive, polar and steric forces on the film surface. That is also the prerequisite for getting a uniform LC alignment. Since the same LC molecules were aligned and a same polymer material was used as the aligning films that showed a similar nanoscaled configuration, it is reasonable to think that the topological part may be the dominant factor that causes the different pretilt angles macroscopically.

According to Berreman's theory, it has been shown that grooved surfaces minimize the elastic deformation energy of the nematic LC molecules by forcing their directors to align parallel to the rubbed grooves or scratches [15]. Through neglecting possible competing anchoring forces from the intermolecular interactions, Berreman showed that the grooved topology of the rubbed surfaces would combine with the inherent tendency of nematics to minimize splay and bend elastic deformations and induce the homogeneous LC alignment. As another topological LC alignment technique, the angular evaporation of SiOx was firstly described by Janning [16]. The SiOx films deposited at different evaporating angles can provide different surface topologies which produce different pretilt angles from 0° to 90° [17 ~ 19].

The glancing-angle deposited needle structure of SiOx films can usually bring about a high pretilt angle.

As we observed on the micrometer scaled AFM image, there existed a needle-like structure on the rubbed film surface. The phenomenon is similar to the case of glancing angle evaporated SiOx where the surface topologies of the evaporated SiOx determines the LC pretilt on it. The LC molecules near the film surfaces have the venture of aligning themselves along the growth direction of the needle-like structure for the energy minimization. While the needle-like structure on the rubbed polymer films has no the roughness and robustness of the evaporated SiOx revealed by AFM [20, 21], the corresponding LC cell only showed a medium pretilt angle of 7°. Seo *et al.*, recently reported that the rubbed polymer films with a high concentration had a higher pretilt angle than that of a low concentration [22]. The topological contribution should be considered because a high sample concentration is liable to form the deformed spherical clusters or some kind of structures alike after the imidization.

The rubbed films aligned nematic LC cells have a stable LC alignment configuration and show no tilt domains even under the electric field. It has also been proved that it is effective to eliminate the zig-zag defects in the SSFLC cells using the rubbed films, which can provide a several degree pretilt angle in the nematic phase, as the aligning layers [23].

To the condition of the PI LB films, there appeared a groovy-like polymer structure mainly along the film depositing direction on the micrometer scale. It is possible that the LC molecules just lie in the grooves and showed a small pretilt angle about 1° along the groovy film surface. It is also a familiar case as on the conventionally rubbed polymer films [2].

As discussed above, we proposed that the dispersive, polar and steric forces induce a uniform LC alignment near the aligning films, while the AFM revealed topological difference determines the final LC pretilt angle. The needle-like structure on the rubbed polymer films plays a major role in producing the oblique LC alignment configuration.

4. CONCLUSIONS

In summary, we fabricated two kinds of PI films to align NLC molecules. The rubbed films aligned LC cell showed a higher pretilt angle than that of aligned by PI LB films. The aligning films were investigated by AFM observation. The AFM images revealed that both kinds of films show an orderly in-line polymer chain structure along either the rubbing direction

or the LB film depositing direction on the nanoscale observation. Scanned under the micrometer scale, the rubbed films have a needle-like structure, while PI LB films show a groovy structure. We explained the most possible underlying factor that causes the different LC alignment on the different method treated films from the view of chemical and physical interactions. We proposed that the intermolecular interactions from the dispersive, polar and steric forces have the main contribution for the uniform alignment of LC molecules along a certain direction that is usually consistent with the employed outer force direction, which is the rubbing direction or the LB film depositing direction, during the films preparation procedure. On the other hand, the AFM revealed microscale topological difference determines the final LC pretilt angle. The needle-like structure on the rubbed PI films is regarded as the dominant factor to determine the pretilt angle and plays the major role in producing the oblique LC alignment configuration.

References

[1] J. Cognard, *Mol. Cryst. and Liq. Cryst.*, **78**, Suppl. 1, 1 (1982).
[2] S. Ishihara, H. Wakemoto, K. Nakazima and Y. Matsuo, *Liq. Cryst.*, **4**, 669 (1989).
[3] M. Murata, H. Awaji, M. Isurugi, M. Uekita and Y. Tawada, *Jpn. J. Appl. Phys.*, **31**, L189 (1992).
[4] H. Ikeno, A. Oh-saki, M. Nitta, N. Ozaki, Y. Yokoyama, K. Nakaya and S. Kobayashi, *Jpn. J. Appl. Phys.*, **27**, L475 (1988).
[5] T. J. Scheffer and J. Nehring, *Appl. Phys. Lett.*, **45**, 1021 (1984).
[6] Y. S. Negi, Y. Suzuki, T. Hagiwara, I. Kawamura, N. Yamamoto, K. Mori, Y. Yamada, M. Kakimoto and Y. Imai, *Liq. Cryst.*, **13**, 153 (1993).
[7] Y. M. Zhu, Z. H. Lu, F. Qian, X. M. Yang and Y. Wei, *Appl. Phys. Lett.*, **63**, 3432 (1993).
[8] Y. M. Zhu, L. Wang, Z. H. Lu, Y. Wei, X. X. Chen and J. H. Tang, *Appl. Phys. Lett.*, **65**, 49 (1994).
[9] Y. B. Kim, H. Olin, S. Y. Park, J. W. Chol, L. Komitov, M. Matuszezyk and S. T. Largerwall, *Appl. Phys. Lett.*, **66**, 2218 (1995).
[10] J. Y. Huang, J. S. Li, Y. S. Juang and S. H. Chen, *Jpn. J. Appl. Phys.*, **34**, 3163 (1995).
[11] T. J. Scheffer and J. Nehring, *J. Appl. Phys.*, **48**, 1783 (1977).
[12] I. Fujiwara, C. Ishimoto and J. Seto, *J. Vac. Sci. Technol. B*, **9**, 1148 (1991).
[13] J. M. Geary, J. W. Goodby, A. R. Kmetz and J. S. Patel, *J. Appl. Phys.*, **62**, 4100 (1987).
[14] K. Okano, N. Matsuura and S. Kobayashi, *Jpn. J. Appl. Phys.*, **21**, L109 (1982).
[15] D. W. Berreman, *Phys. Rev. Lett.*, **28**, 1683 (1972).
[16] L. Janning, *Appl. Phys. Lett.*, **21**, 173 (1972).
[17] L. A. Goodman, J. T. Mcginn, C. H. Anderson and F. Digeronimo, *IEEE Transactions on Electron Devices*, **24**, 795 (1977).
[18] M. Monkade, M. Boix and G. Durand, *Europhys. Lett.*, **5**, 697 (1988).
[19] M. Murate, M. Uekita, Y. Nakajima and K. Saitoh, *Jpn. J. Appl. Phys.*, **32**, L679 (1993).
[20] H. Vithana, D. Johnson, A. Alberict and J. Lando, *Jpn. J. Appl. Phys.*, **34**, L131 (1995).
[21] H. Vithana, D. Johnson and P. Bos, *Jpn. J. Appl. Phys.*, **35**, L320 (1996).
[22] D. S. Seo and S. Kobayashi, *Jpn. J. Appl. Phys.*, **34**, L786 (1995).
[23] R. B. Lu, K. S. Xu, Y. K. Le, H. H. Deng, N. Gu and Z. H. Lu, accepted in, *Jpn. J. Appl. Phys.* (1997).